Radial migration in the Galactic disc with a decelerating bar

— Signatures in the disc’s chemical cartography

Hanyuan Zhang (hz420@cam.ac.uk)

Collaborators: Vasily Belokurov, N. Wyn Evans, Jason L. Sanders, Yuxi(Lucy) Lu, Changye Cao, GyuChul Meyong, Adam Dillamore, Sarah G. Kane , Zhao-Yu Li

ioa

UNIVERSITY OF CAMBRIDGE
Institute of Astronomy

Zhang H. et al., 2025, ApJL, 983, L10

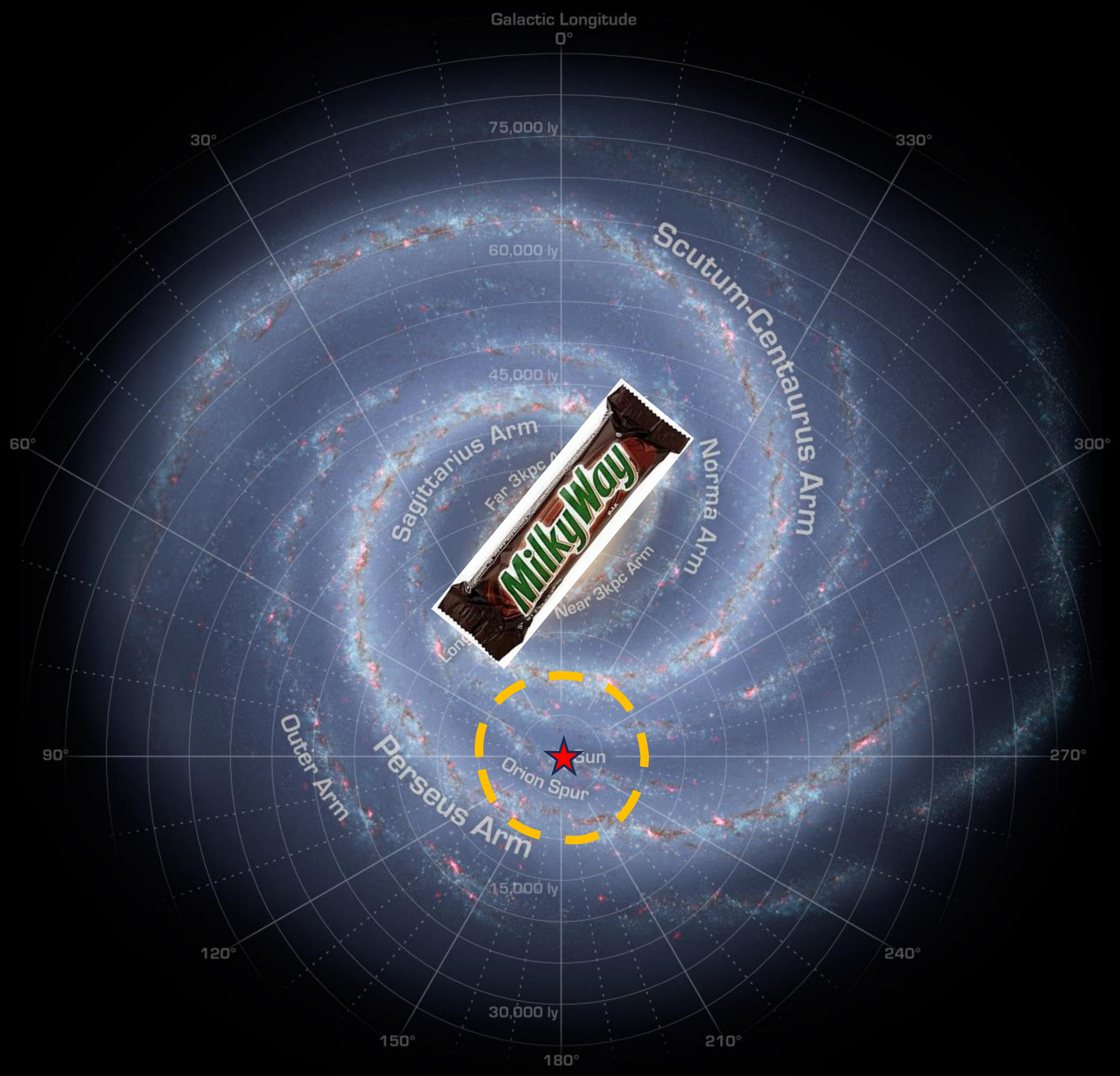

For stars in the solar neighbourhood, we can measure their:

- Kinematics
- Metallicity
- Chemical abundances
- Ages

Where were these stars born in the Milky Way?

Stellar migrations in the Galactic disc

- Stars could move from their birth radius to their present-day radius, called radial migration

- This process happens through interaction with non-axisymmetric perturbations, e.g. the transient spiral arms, galactic bar.

See Sellwood & Binney 02, Minchev & Famaey 10, Halle +15

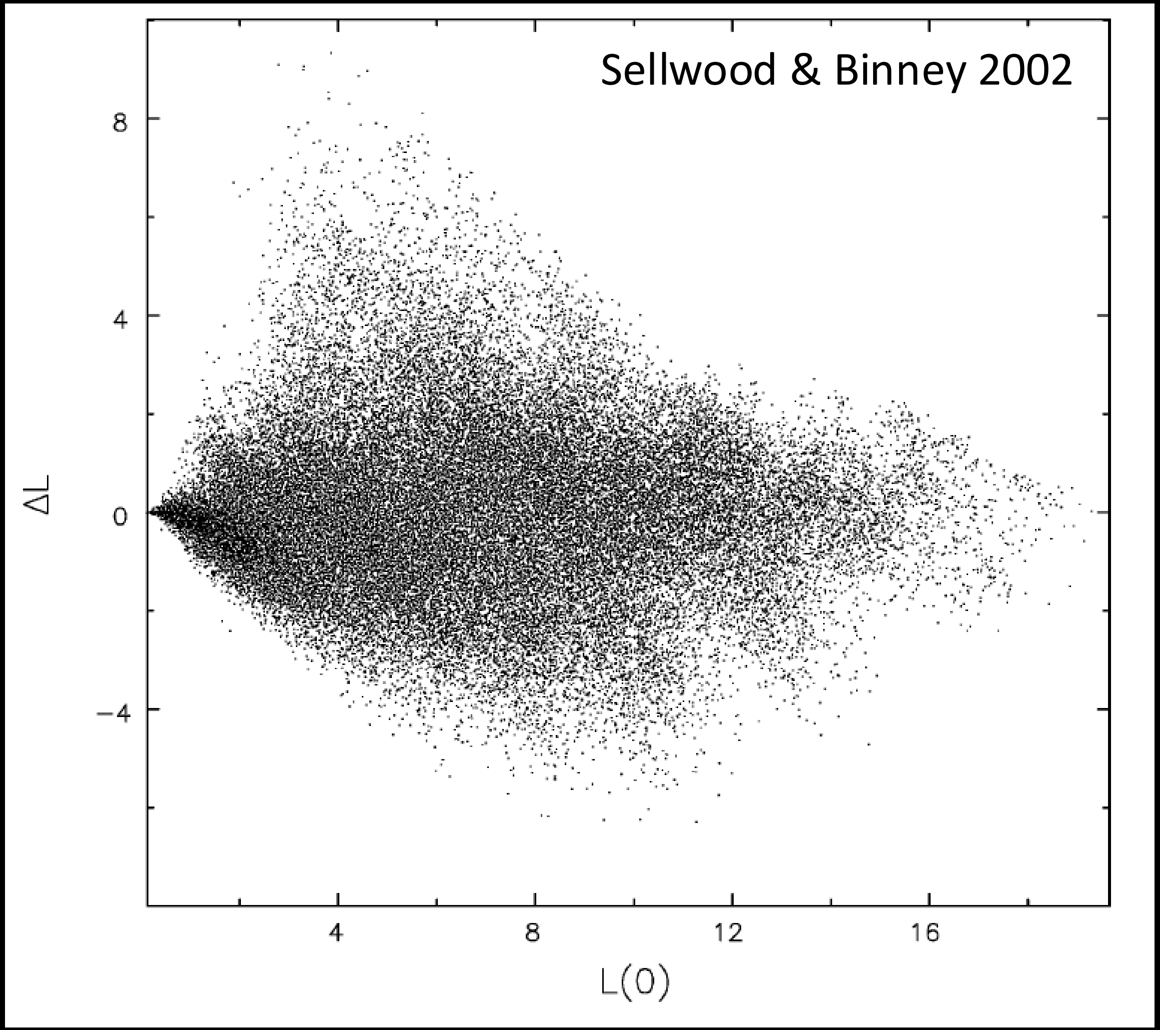

Observational evidence of radial migration

- As the Galactic ISM are axisymmetric within $\lesssim$0.1 dex (Wenger+19, etc.), the observed stellar metallicity in the solar neighbourhood should have little spread at each ages.

- The large metallicity spread in the stellar metallicity at each age reflects the amount of radial migration in the Galactic disc.

$$\delta L_z \sim \frac{V_c \, \sigma_{[\mathrm{Fe/H}]}}{|d[\mathrm{Fe/H}]/dR|}$$

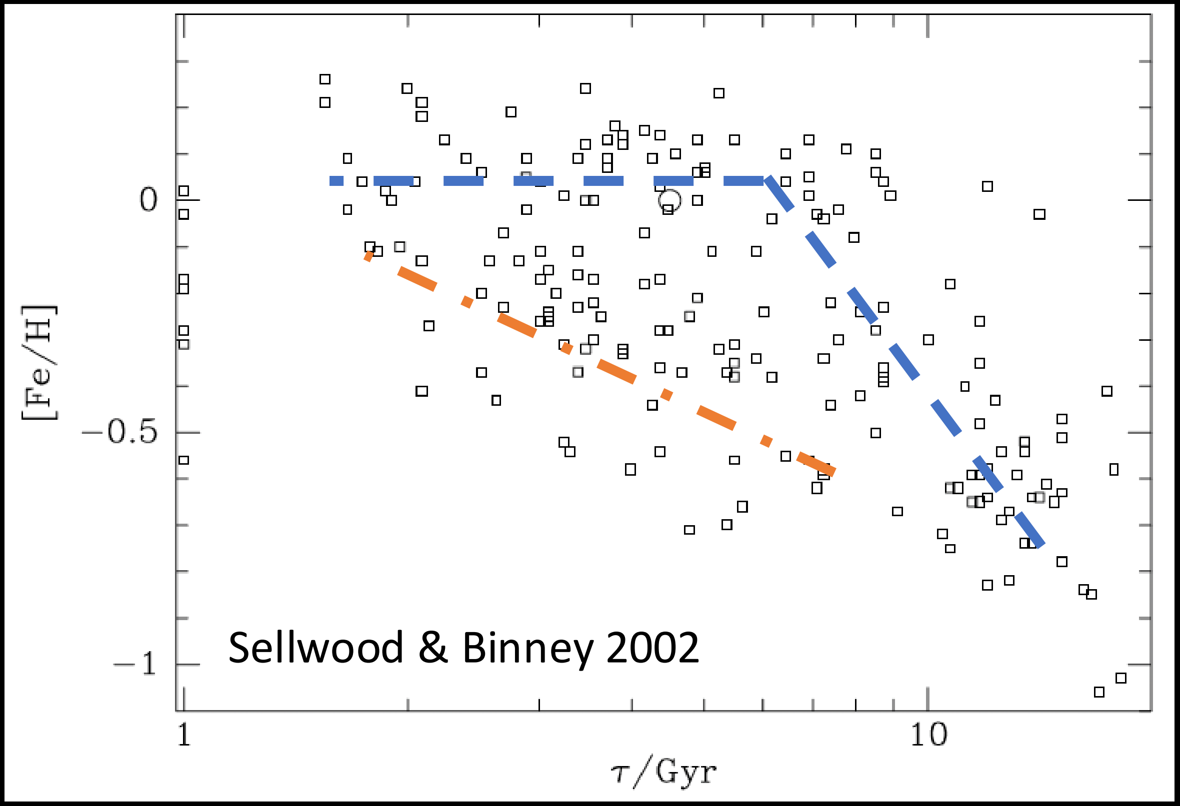

$\delta R \sim 3.5\ \mathrm{kpc}\ \sqrt{\tau/8\ \mathrm{Gyr}}$ from Frankel+18

See Sellwood & Binney 02, Frankel+20

Chemical cartography in the Galactic disc

The age-metallicity plane

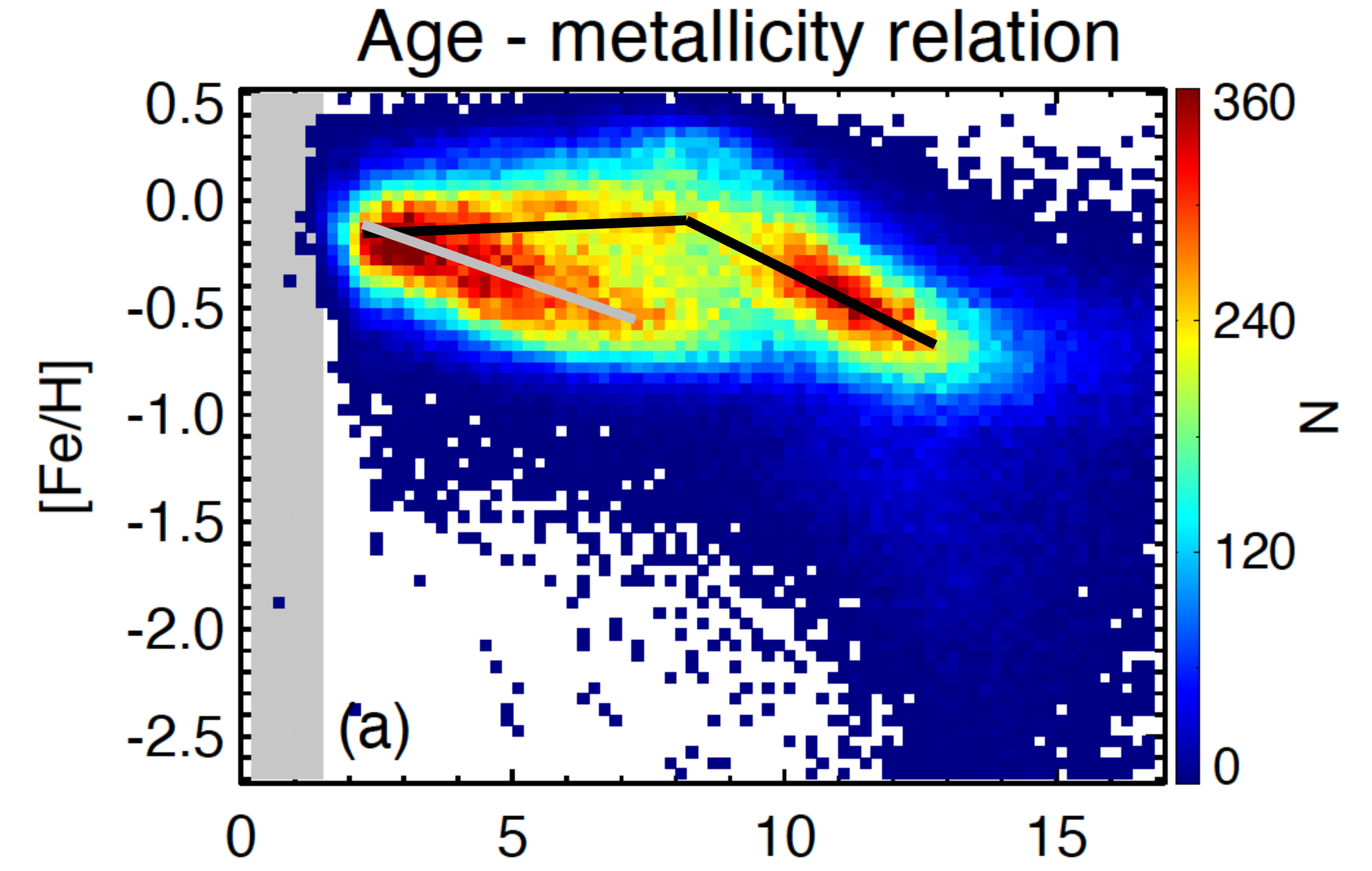

Xiang & Rix 2022

Question:

What mechanism caused this bimodal sequences

&

What can we learn about the past of the Milky Way from this

Resonant dragging of a decelerating bar

A tov demonstration

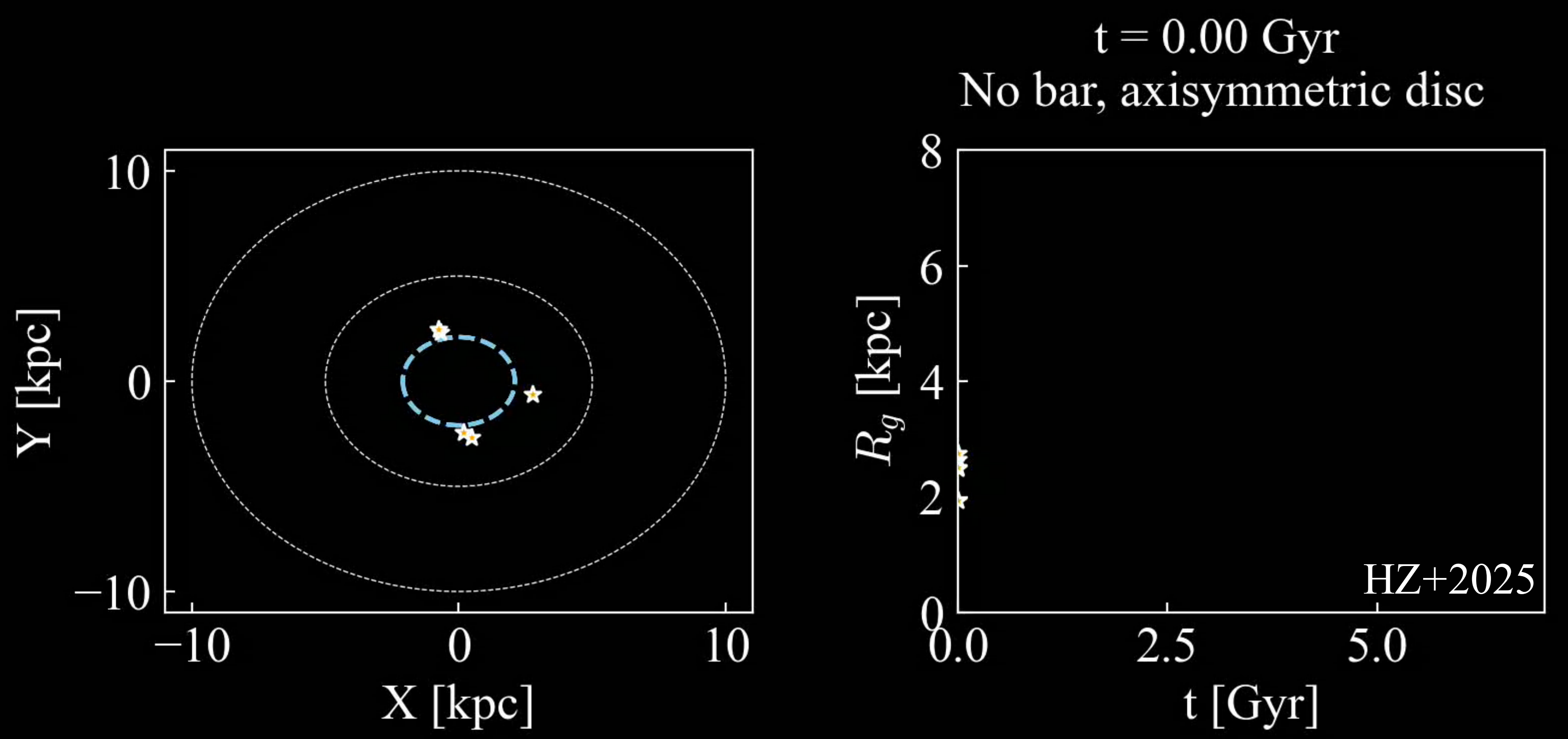

Stars trapped in the corotation resonance migrate with the expansion of the corotation. This brings stars from the inner Milky Way to the present-day corotation radius.

See Chiba+21; Chiba & Schonrich 2021 for analytic descriptions and very beautiful figures

Today's pattern speed ~ 32 – 37 km/s/kpc (Chiba+21, Clarke+22, Zhang+24, Dillamore+24,25); corotation radius ~ 6.5 – 7.5 kpc

Resonant dragging of a decelerating bar

Test-particle simulation setup

Initialise a quasi-isothermal disc in an axisymmetric disc potential

Grow a galactic bar in the background potential with an initial pattern speed $\Omega_i = 80$ km/s/kpc ($R_{CR,init} \sim 2.7$ kpc)

Bar reach its maximum strength and start decelerate with $\eta = -\dot{\Omega}/\Omega^2 = 0.003$

Deceleration stop when it reaches the present-day pattern speed $\Omega_0 = 34$ km/s/kpc ($R_{CR,0} \sim 6.5$ kpc)

t = 0 Gyr — t = 3.5 Gyr — t = 4.5 Gyr — 11.5 Gyr

Add new disc stellar particles into the simulation constantly with time

Assign metallicity to the test particles afterwards with a model $[\mathrm{Fe/H}] = f(R_b, \tau)$

Cut $d_{Sun} < 3$ kpc to mimic the coverage of the subgiant sample

Resulting age-metallicity sequences

Local stars vs. migrated stars

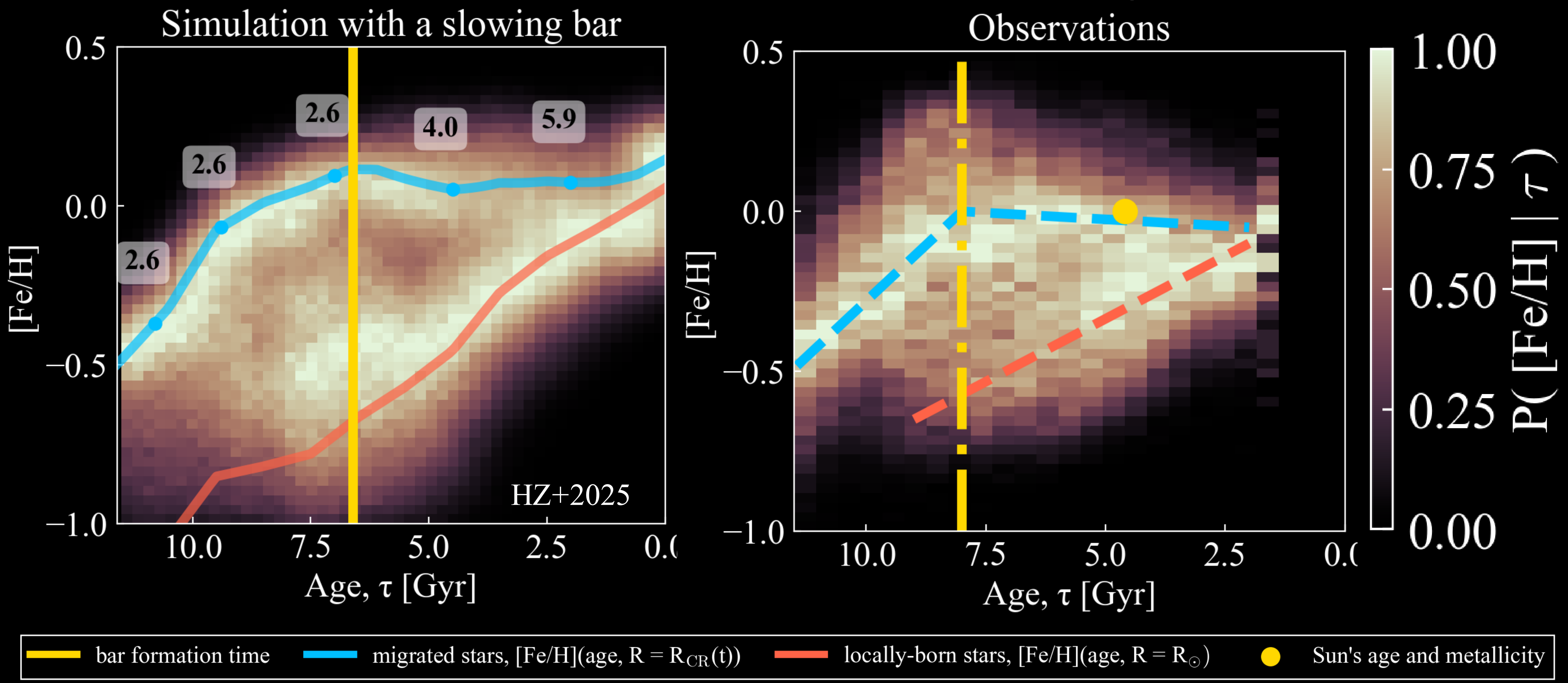

Resulting age-metallicity sequences

Local stars vs. migrated stars

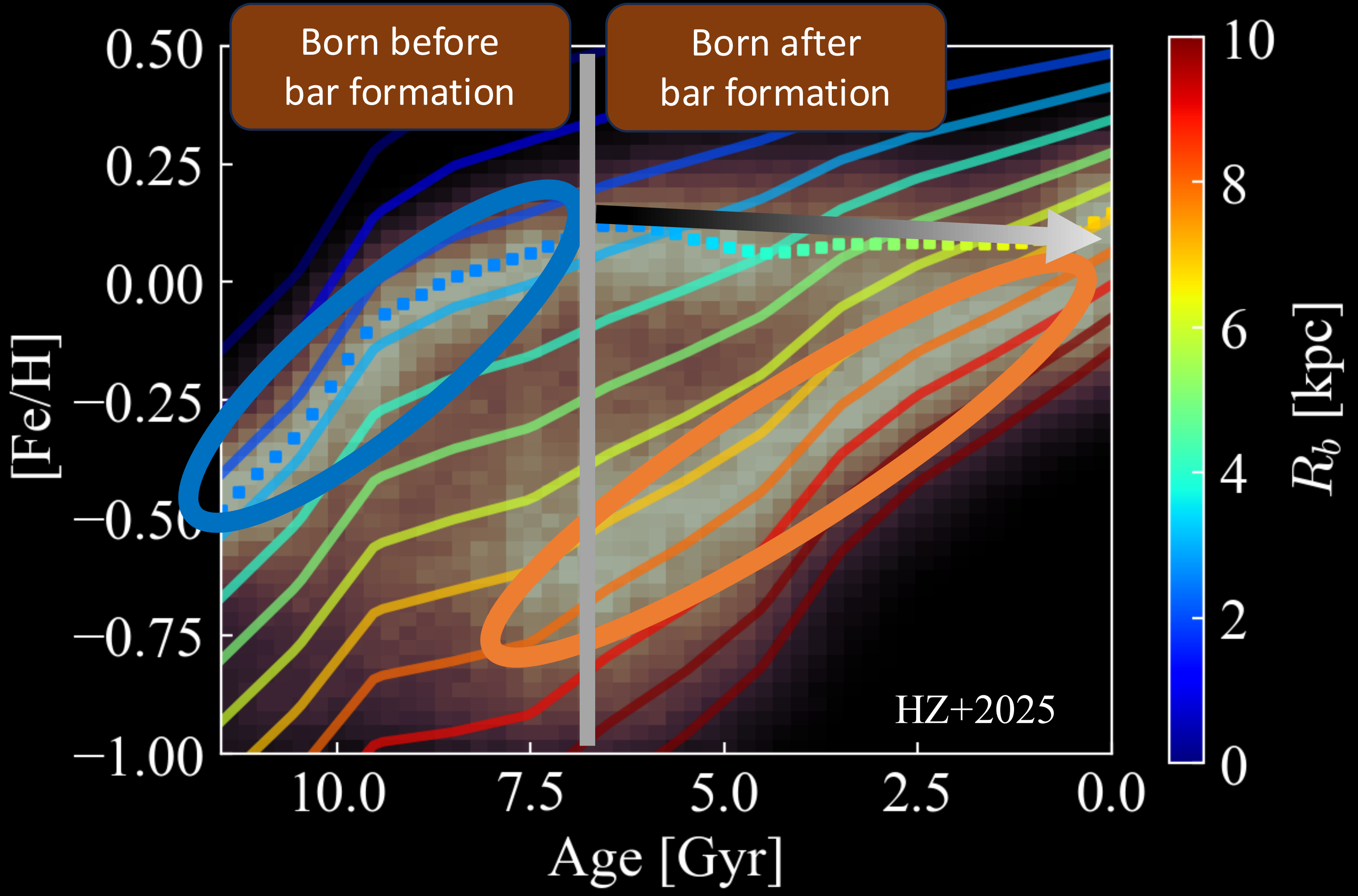

Stars born ***before bar formation***: those that has $R_b \sim R_{CR,\,init}$ experience strong resonance dragging

Age-metallicity sequence tracks [Fe/H]$(\tau, R_b \sim R_{CR,\,init})$

Stars born ***after bar formation:*** those that has $R_b \sim R_{CR}(t = \tau)$ experience strong resonance dragging

Age-metallicity sequence flattens, and tracks [Fe/H]$(\tau, R_b \sim R_{CR,\,\tau})$

Resulting age-metallicity sequences

The guiding radii dependence

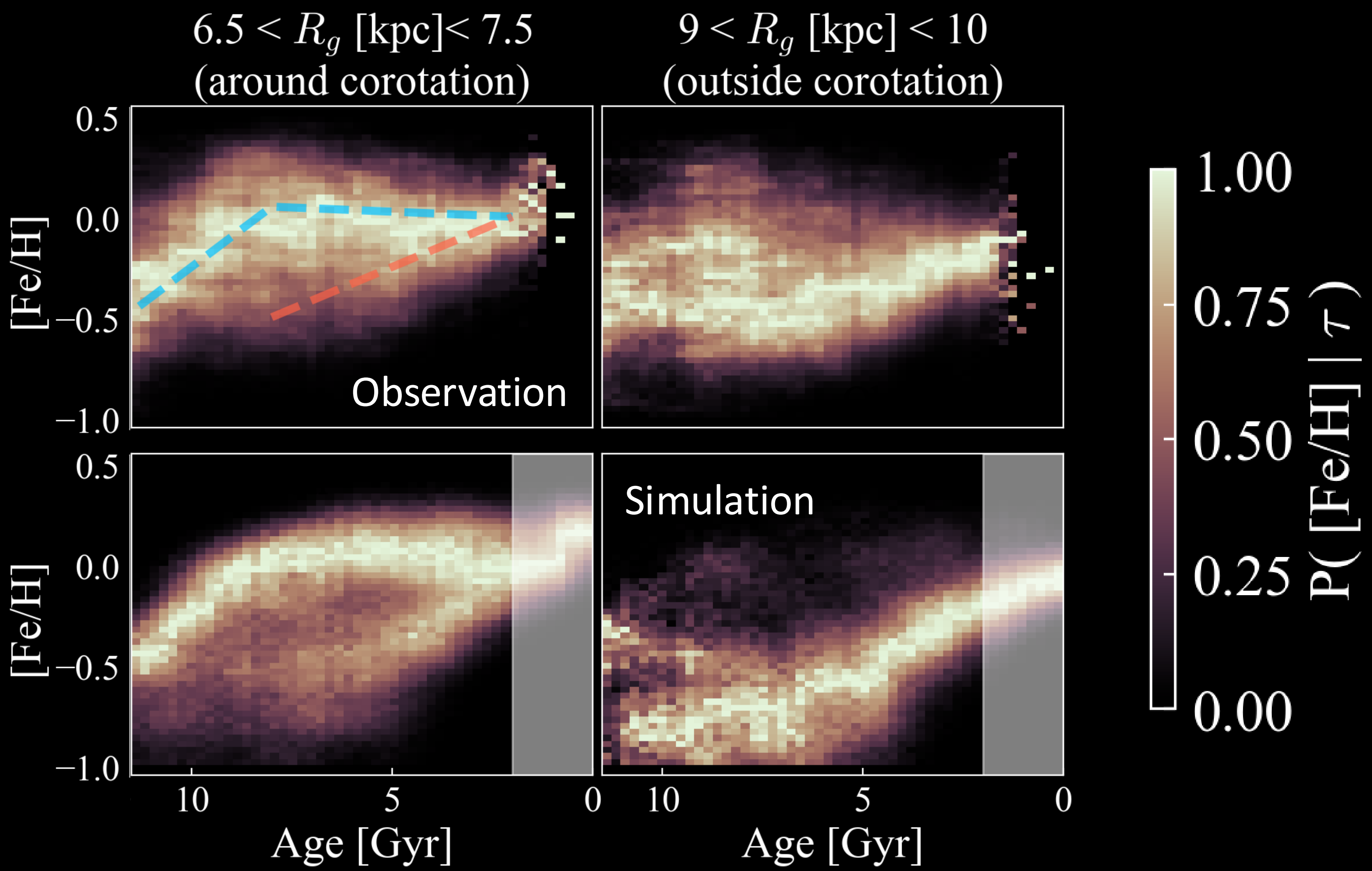

HZ+2025

Resulting age-metallicity sequences

The guiding radii dependence

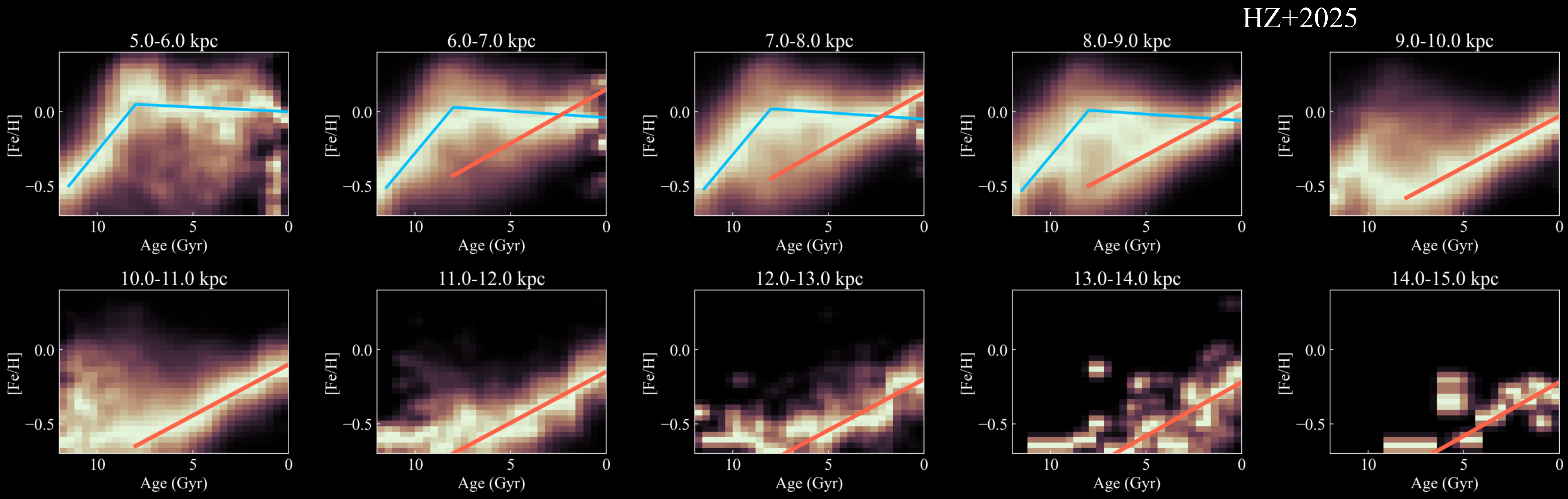

Resulting age-metallicity sequences

The guiding radii dependence

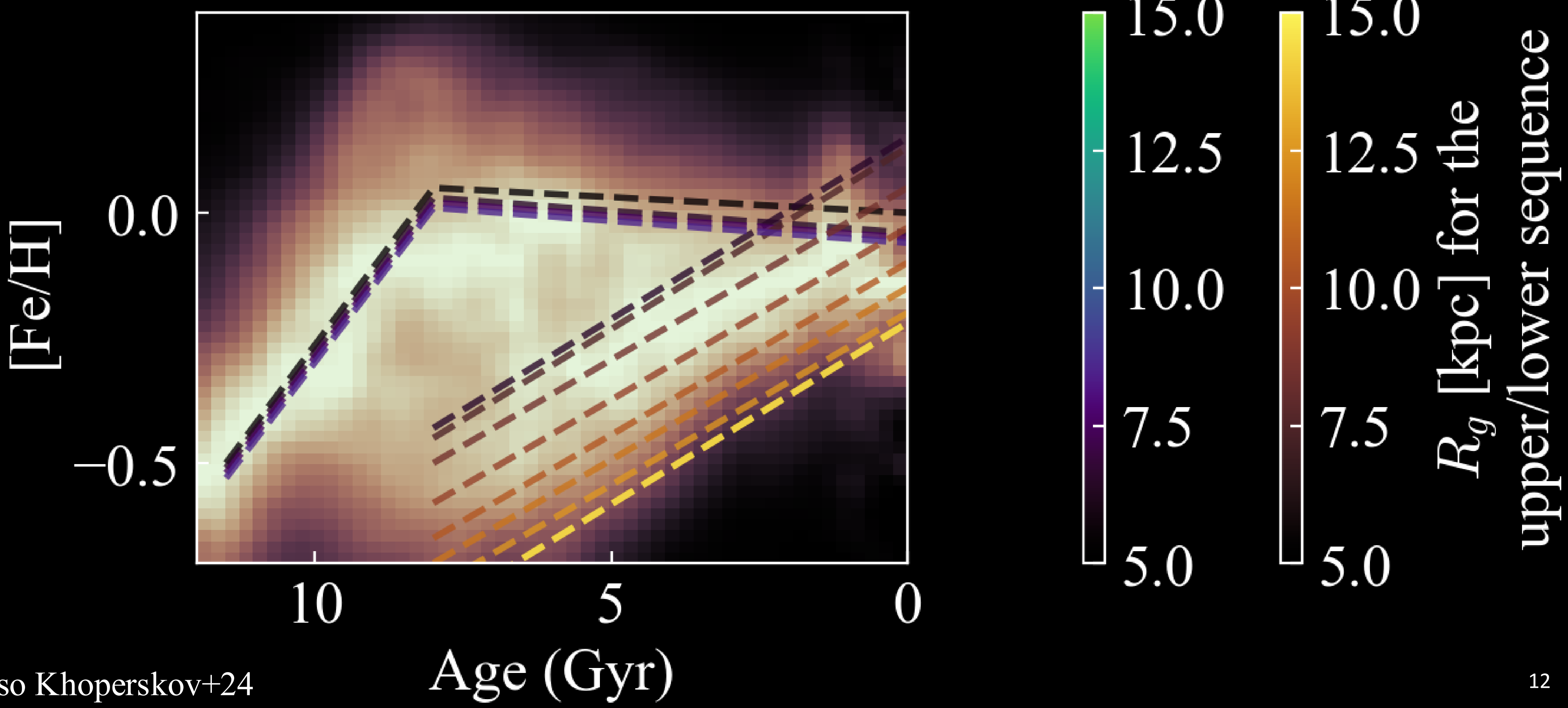

See also Khoperskov+24

Implications: 1) $[\alpha/\mathrm{Fe}] - [\mathrm{Fe/H}]$ bimodality

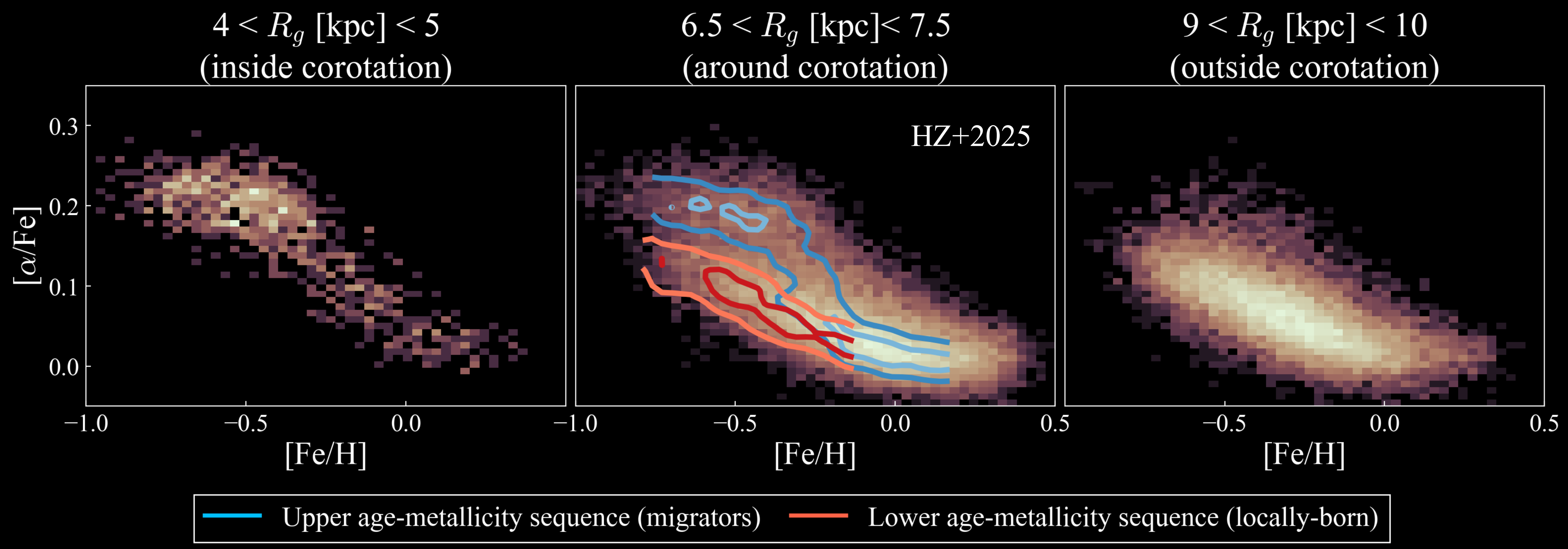

See more detailed chemical cartography map in Hayden+15

See also Sharma+21

Inferring the pattern speed history of the bar

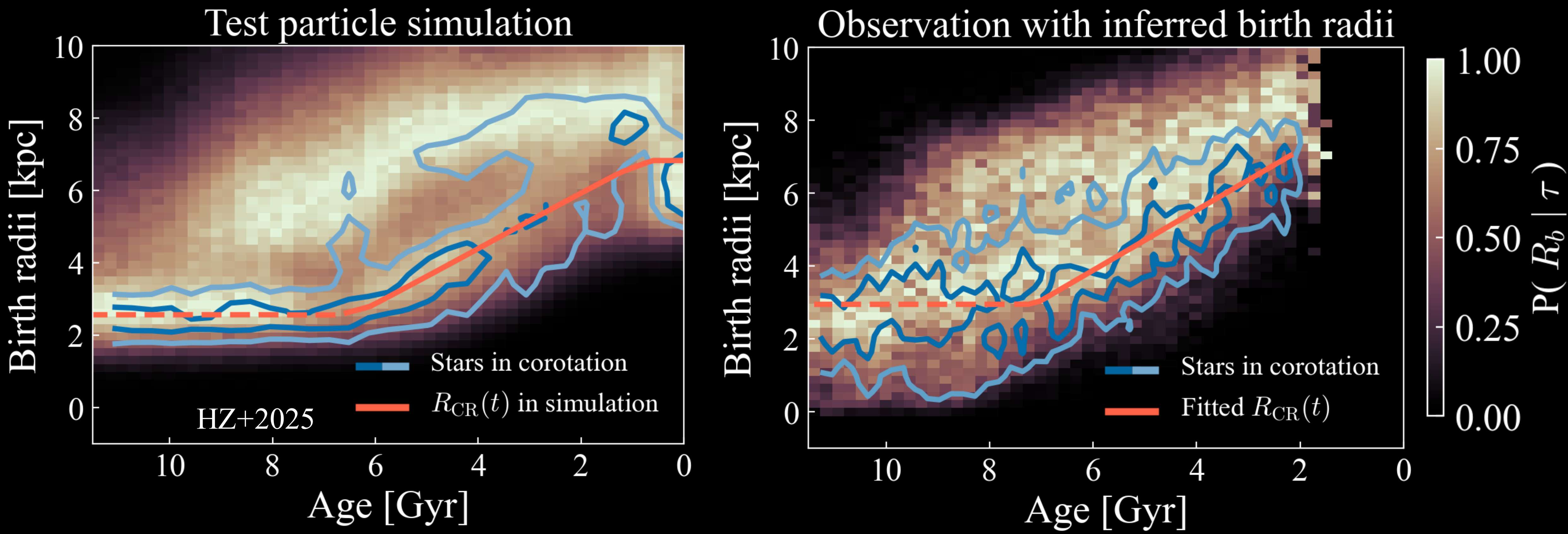

In this birth radius calculation method (Lu+24), we can infer:

$$t_{bf} \sim 6 - 8 \text{ Gyr}; \Omega_i \sim 60 - 100 \text{ km/s/kpc}; \eta = -\dot{\Omega}/\Omega^2 \sim 0.0025 - 0.004$$

agree with other independent measurements of t_{bf} and η (Chiba+21, Sanders+24), and non-independently Haywood+24

Zhang H. et al., 2025,
ApJL *accepted*

Conclusion

- The Milky Way's age-metallicity distribution shows two distinct sequences, and exhibit clear transition as a function of R_g

- We interpret the two distinct sequences as they consist ***migrated stars*** and ***locally-born stars***, respectively, in which the migrated stars are driven by the corotation resonance dragging of the decelerating bar.

- This interpretation could also help to explain the disc's α-bimodality and its guiding radii dependence, the observed azimuthal chemical patterns, the broken stellar density distribution, and the coldness of the disc.

- In this scenario, we could infer the pattern speed history of the Galactic bar. We obtained $t_{bf}\sim 6-8$ Gyr; $\Omega_i\sim 60-100$ km/s/kpc; $\eta=-\dot{\Omega}/\Omega^2\sim 0.0025-0.004$

Resonant dragging of a decelerating bar

A quick introduction

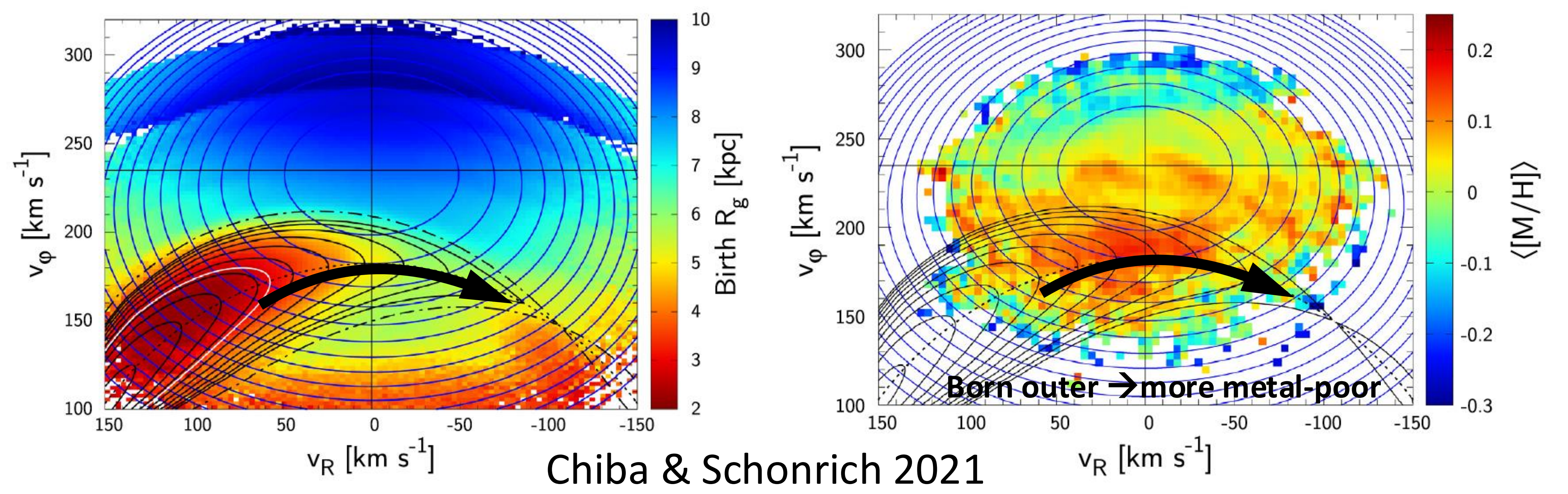

Chiba & Schonrich 2021

Today's bar pattern speed: $\Omega_b \sim 33 - 37$ km/s/kpc (Chiba+21; Clarke+22; Zhang+24 ; Dillamore+24, 25) → Corotation radius $R_{CR} \sim 6.2 \ - 7.0$ kpc

Resonant dragging of a decelerating bar

Test-particle simulation setup

This is adopted from Lu+24, which calibrated with observed Milky Way's metallicity pattern

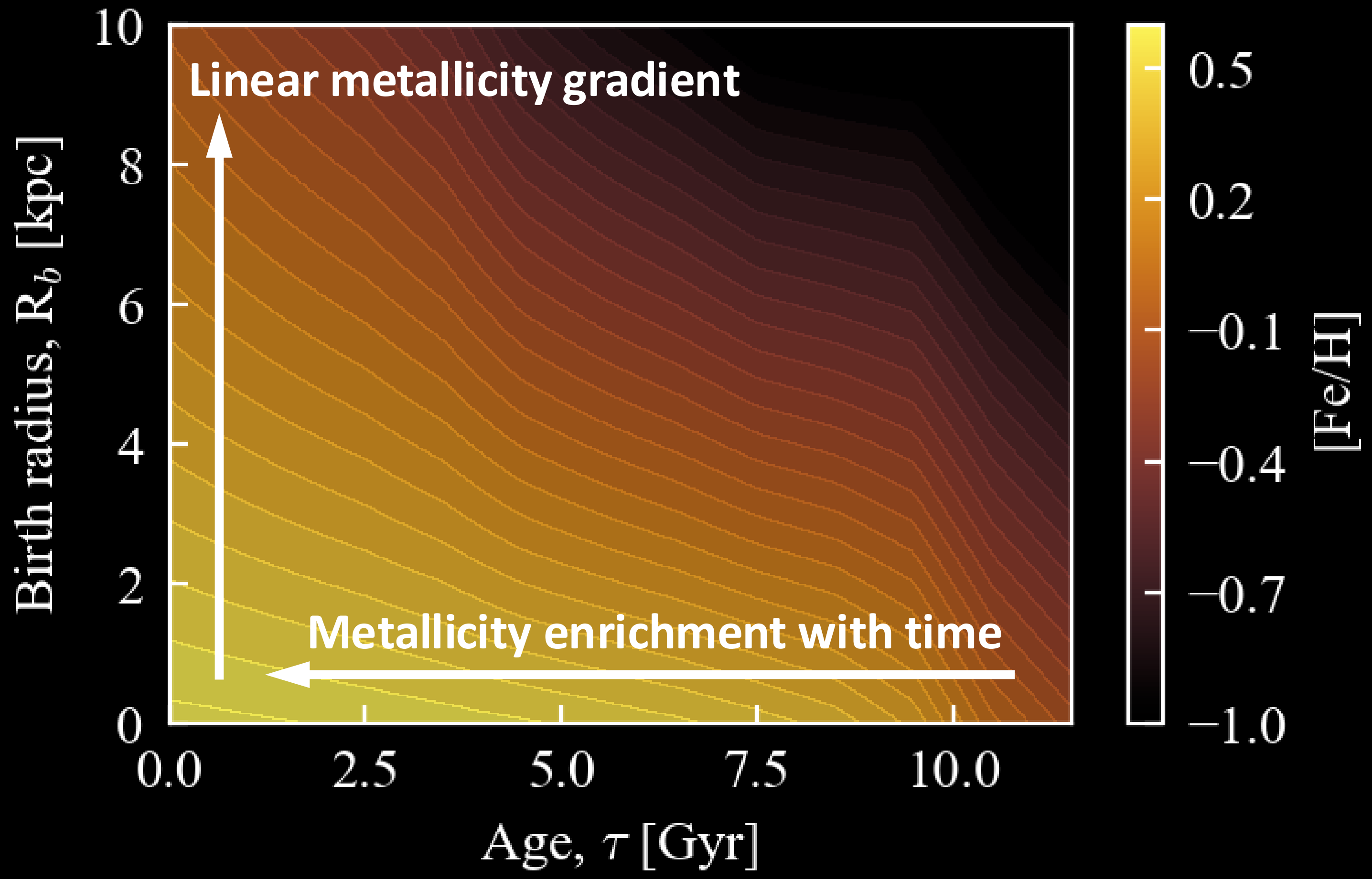

Implications: 3) Broken power-law in stellar density

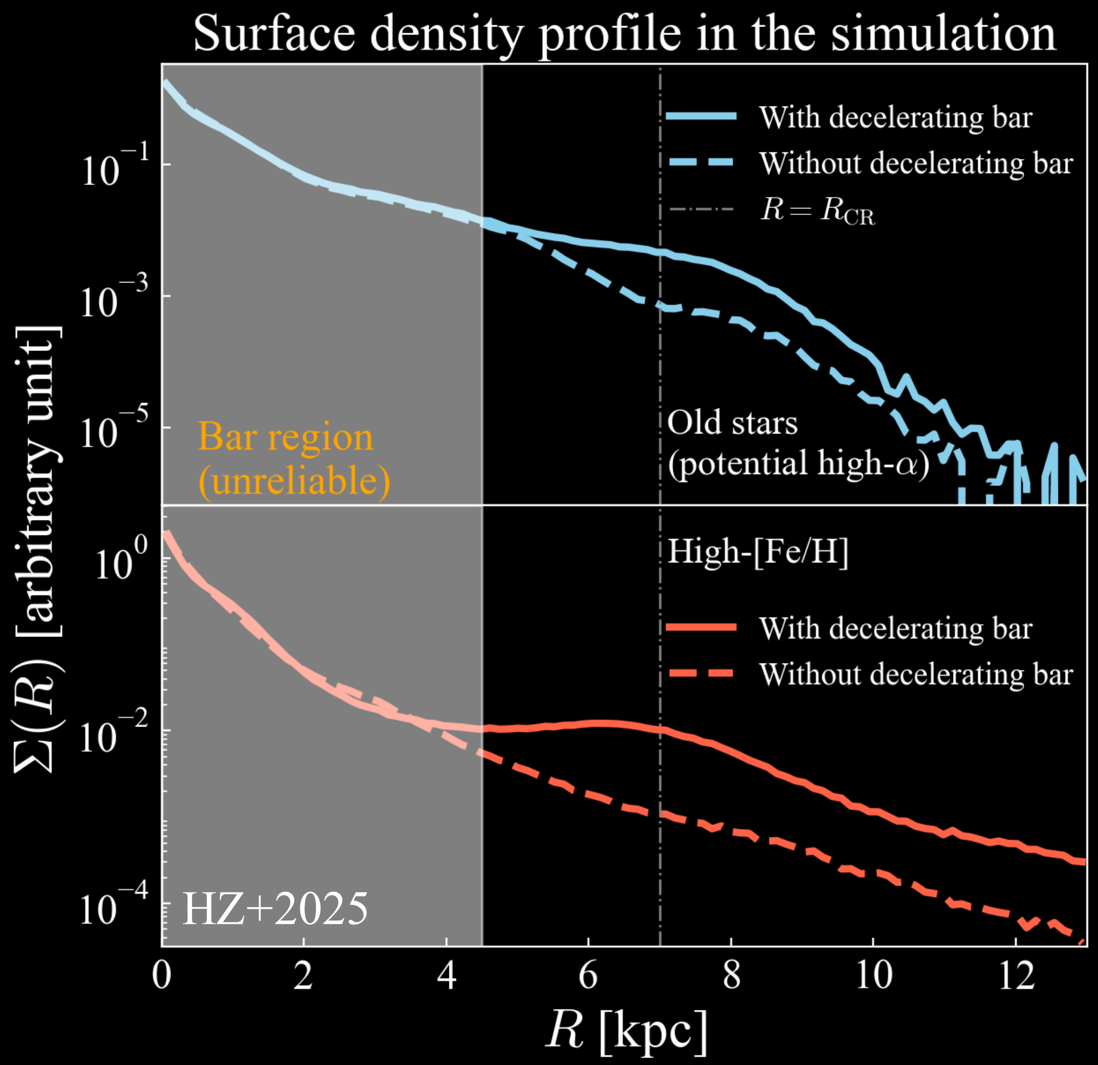

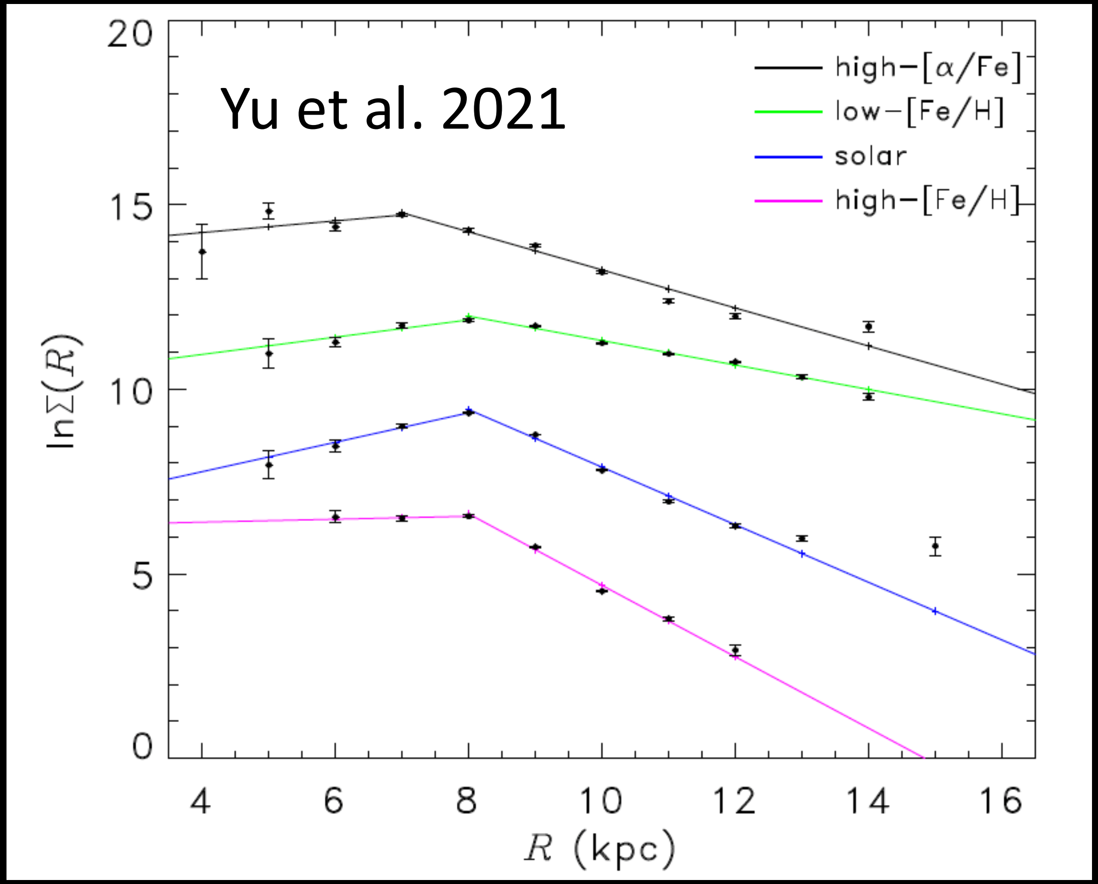

See also Bovy+15, Lian+22

Implications: 4) Coldness of the disc

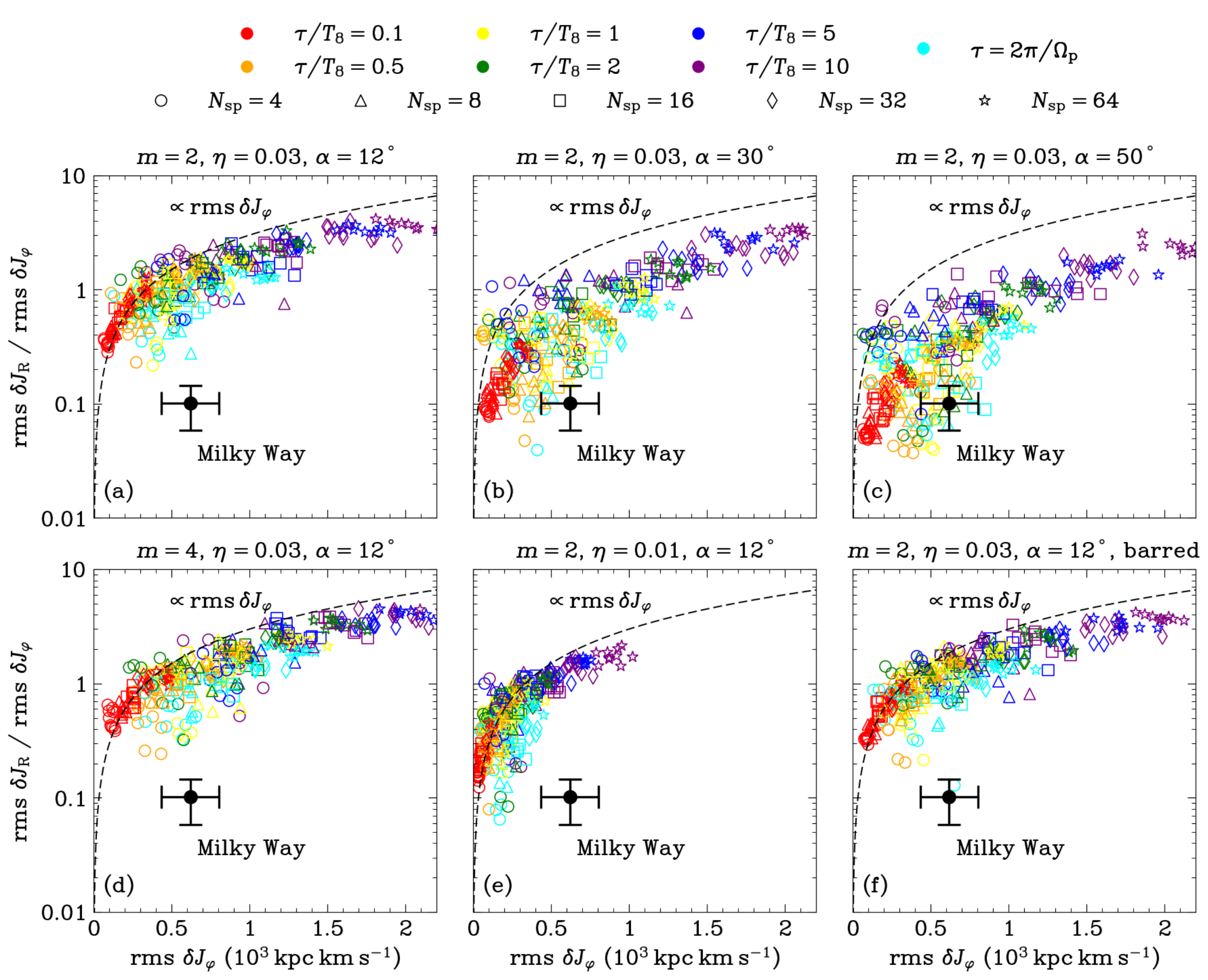

Hamilton et al. 2024

The Milky Way observation is from Frankel+20

But see also the demonstration in Sellwood & Binney 2025

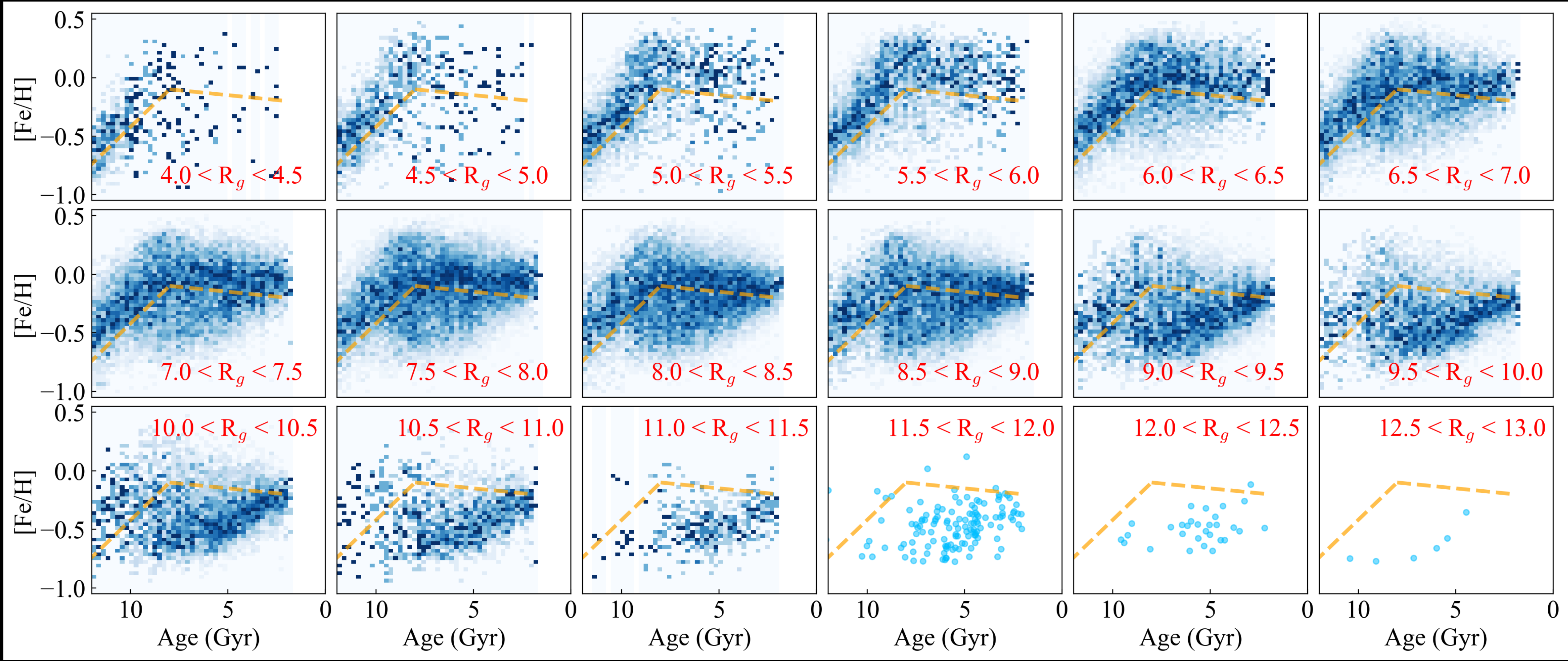

[Fe/H]
Age (Gyr)
4.0 < R_g < 4.5
4.5 < R_g < 5.0
5.0 < R_g < 5.5
5.5 < R_g < 6.0
6.0 < R_g < 6.5
6.5 < R_g < 7.0
7.0 < R_g < 7.5
7.5 < R_g < 8.0
8.0 < R_g < 8.5
8.5 < R_g < 9.0
9.0 < R_g < 9.5
9.5 < R_g < 10.0
10.0 < R_g < 10.5
10.5 < R_g < 11.0
11.0 < R_g < 11.5
11.5 < R_g < 12.0
12.0 < R_g < 12.5
12.5 < R_g < 13.0

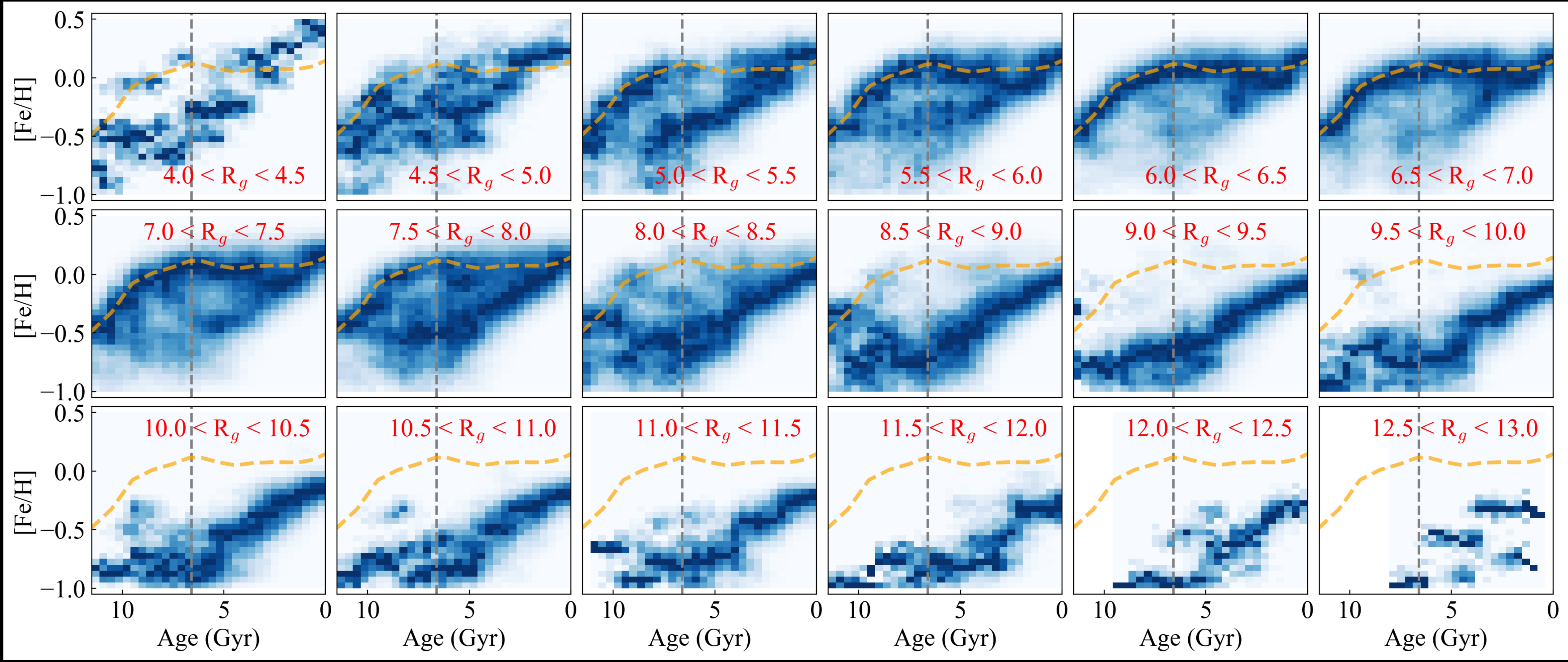

[Fe/H]
0.5
0.0
−0.5
−1.0
Age (Gyr)
10
5
0
4.0 < R_g < 4.5
4.5 < R_g < 5.0
5.0 < R_g < 5.5
5.5 < R_g < 6.0
6.0 < R_g < 6.5
6.5 < R_g < 7.0
7.0 < R_g < 7.5
7.5 < R_g < 8.0
8.0 < R_g < 8.5
8.5 < R_g < 9.0
9.0 < R_g < 9.5
9.5 < R_g < 10.0
10.0 < R_g < 10.5
10.5 < R_g < 11.0
11.0 < R_g < 11.5
11.5 < R_g < 12.0
12.0 < R_g < 12.5
12.5 < R_g < 13.0

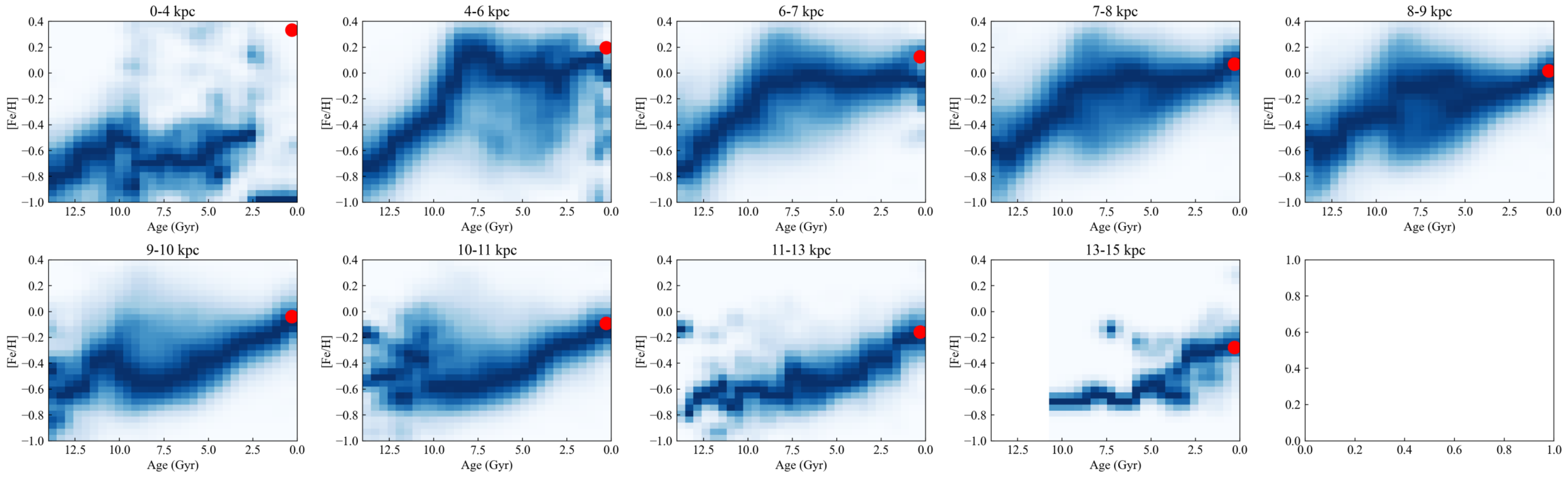
0-4 kpc
4-6 kpc
6-7 kpc
7-8 kpc
8-9 kpc
9-10 kpc
10-11 kpc
11-13 kpc
13-15 kpc
[Fe/H]
Age (Gyr)

Implications: 2) Azimuthal patterns

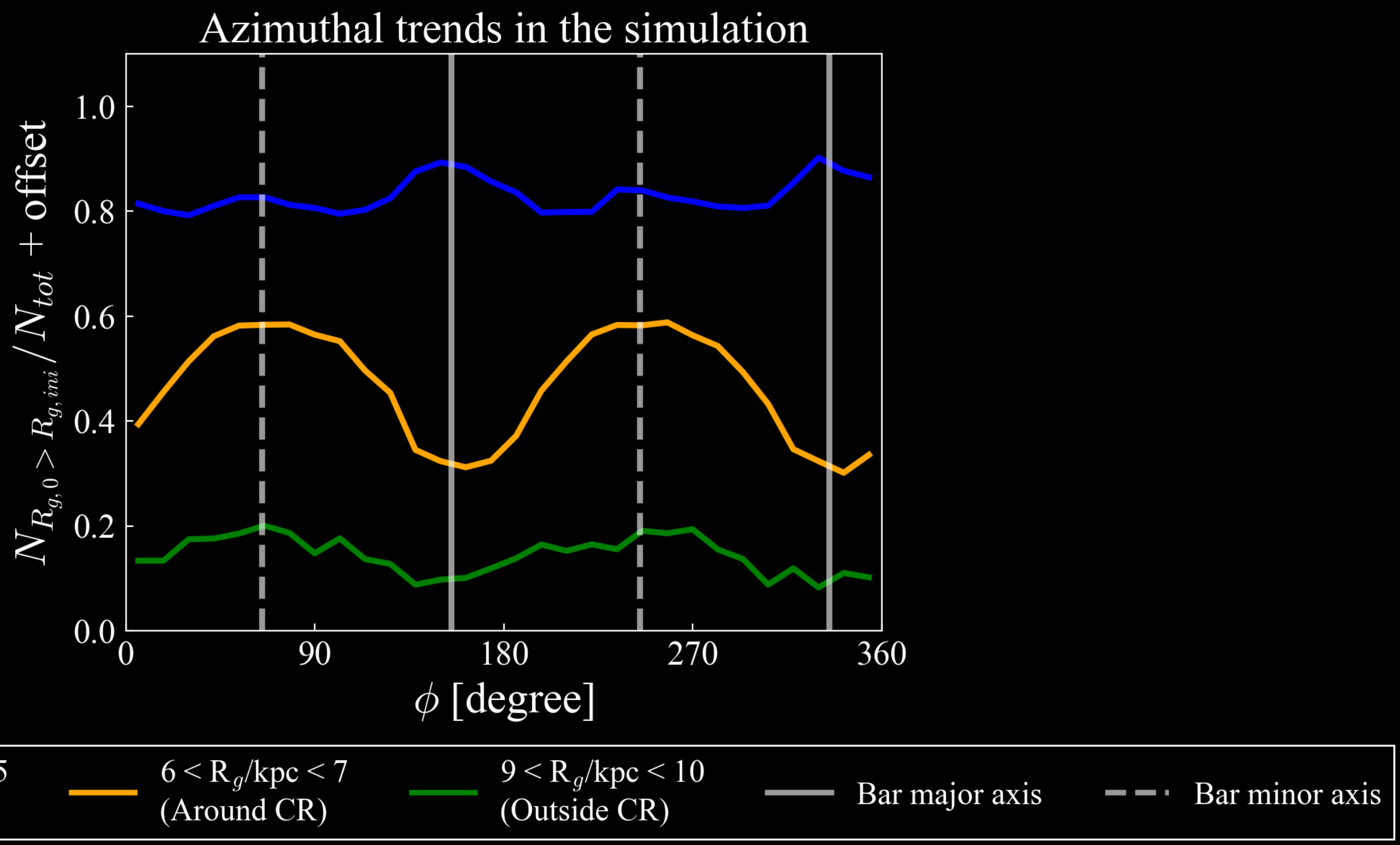

HZ+2025

Implications: 2) Azimuthal patterns

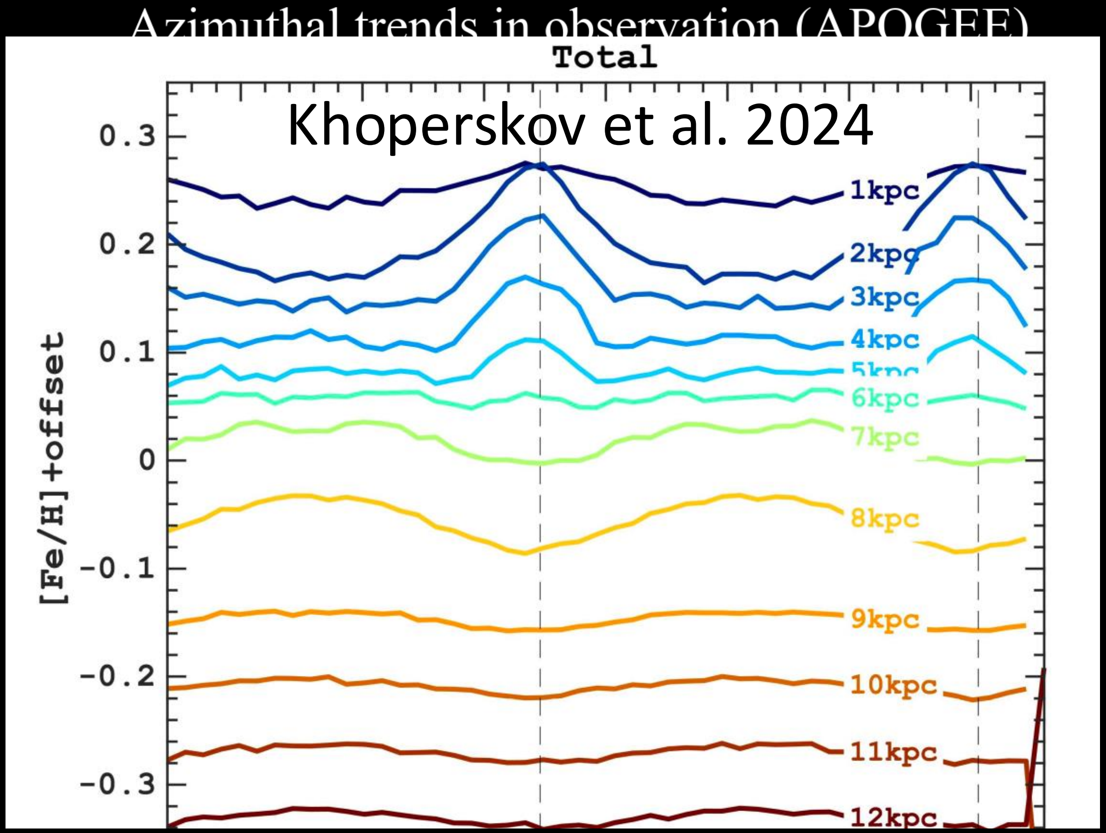

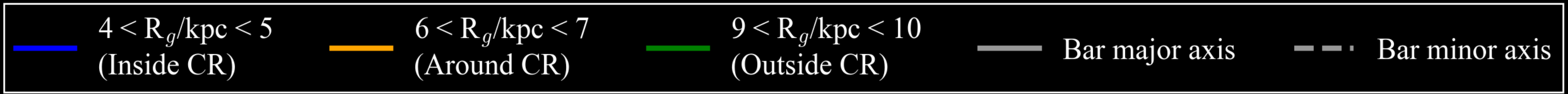

HZ+2025

See also Poggio+23, Hawkins 2023, Hackshaw+24

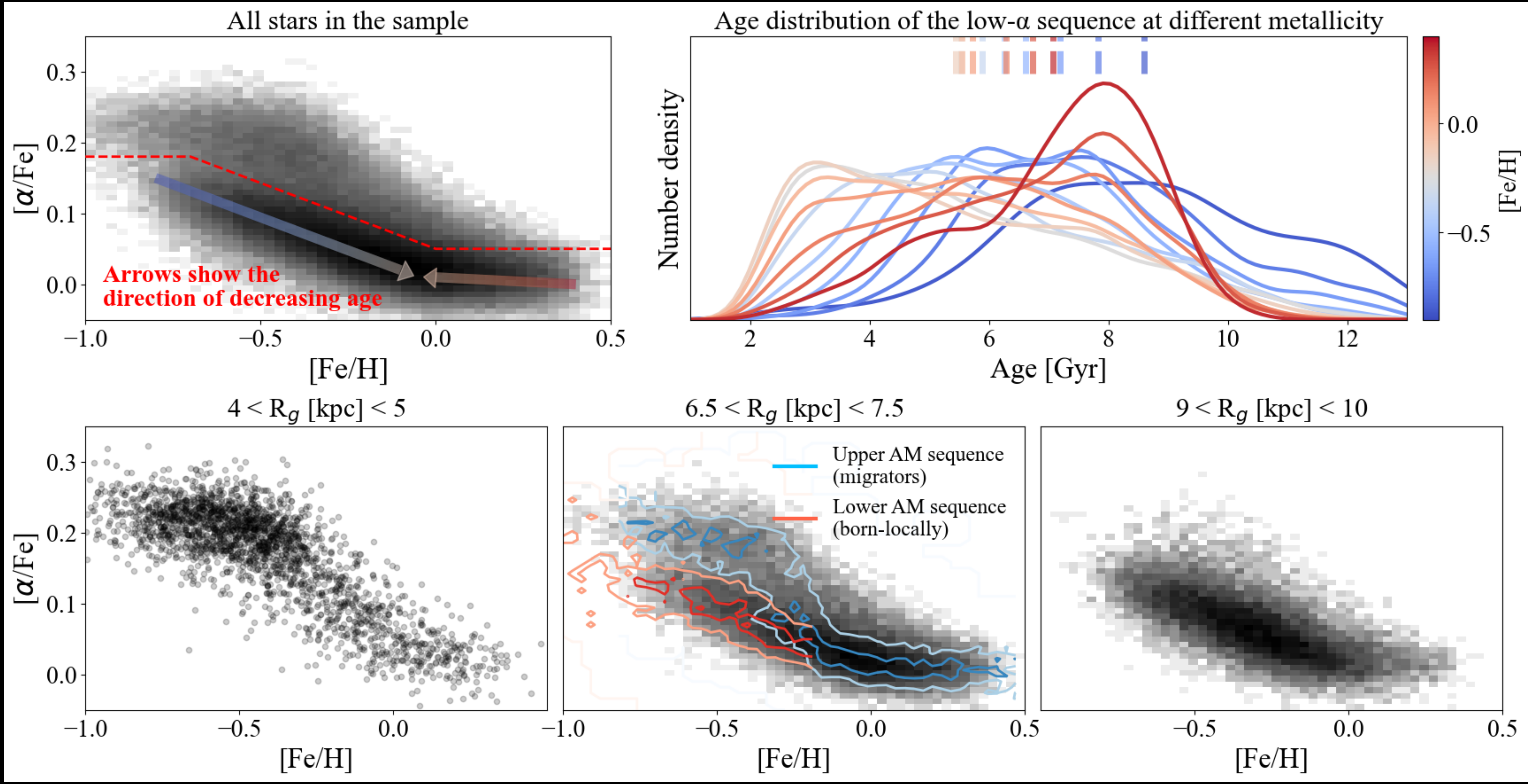
All stars in the sample
[α/Fe]
[Fe/H]
Arrows show the direction of decreasing age
Age distribution of the low-α sequence at different metallicity
Number density
Age [Gyr]
[Fe/H]
4 < R_g [kpc] < 5
6.5 < R_g [kpc] < 7.5
9 < R_g [kpc] < 10
Upper AM sequence (migrators)
Lower AM sequence (born-locally)